

High-fidelity topological quantum state transfers in a cavity-magnon system

Xi-Xi Bao(包茜茜), Gang-Feng Guo(郭刚峰), Xu Yang(杨煦), and Lei Tan(谭磊)

Citation: Chin. Phys. B, 2023, 32 (**8**): 080301. DOI: 10.1088/1674-1056/acc3f6
Journal homepage: http://cpb.iphy.ac.cn; http://iopscience.iop.org/cpb

What follows is a list of articles you may be interested in

Engineering topological state transfer in four-period Su-Schrieffer-Heeger chain

Xi-Xi Bao(包茜茜), Gang-Feng Guo(郭刚峰), and Lei Tan(谭磊)
Chin. Phys. B, 2023, 32 (**2**): 020301. DOI: 10.1088/1674-1056/ac7bfe

Interaction induced non-reciprocal three-level quantum transport

Sai Li(李赛), Tao Chen(陈涛), Jia Liu(刘佳), and Zheng-Yuan Xue(薛正远)
Chin. Phys. B, 2021, 30 (**6**): 060314. DOI: 10.1088/1674-1056/abee0c

Dissipative generation for steady-state entanglement of two transmons in circuit QED

Shuang He(何爽), Dan Liu(刘丹), Ming-Hao Li(李明浩)
Chin. Phys. B, 2019, 28 (**8**): 080303. DOI: 10.1088/1674-1056/28/8/080303

Spin manipulation in semiconductor quantum dots qubit

Ke Wang(王柯), Hai-Ou Li(李海欧), Ming Xiao(肖明), Gang Cao(曹刚), Guo-Ping Guo(郭国平)
Chin. Phys. B, 2018, 27 (**9**): 090308. DOI: 10.1088/1674-1056/27/9/090308

Qubits based on semiconductor quantum dots

Xin Zhang(张鑫), Hai-Ou Li(李海欧), Ke Wang(王柯), Gang Cao(曹刚), Ming Xiao(肖明), Guo-Ping Guo(郭国平)
Chin. Phys. B, 2018, 27 (**2**): 020305. DOI: 10.1088/1674-1056/27/2/020305

High-fidelity topological quantum state transfers in a cavity–magnon system

Xi-Xi Bao(包茜茜)[1], Gang-Feng Guo(郭刚峰)[1], Xu Yang(杨煦)[1], and Lei Tan(谭磊)[1,2,†]

[1] *Lanzhou Center for Theoretical Physics, Key Laboratory of Theoretical Physics of Gansu Province, Lanzhou University, Lanzhou* 730000, *China*
[2] *Key Laboratory for Magnetism and Magnetic Materials of the Ministry of Education, Lanzhou University, Lanzhou* 730000, *China*

(Received 12 December 2022; revised manuscript received 3 March 2023; accepted manuscript online 14 March 2023)

We propose a scheme for realizing high-fidelity topological state transfer via the topological edge states in a one-dimensional cavity–magnon system. It is found that the cavity–magnon system can be mapped analytically into the generalized Su–Schrieffer–Heeger model with tunable cavity–magnon coupling. It is shown that the edge state can be served as a quantum channel to realize the photonic and magnonic state transfers by adjusting the coupling strength between adjacent cavity modes. Further, our scheme can realize the quantum state transfer between photonic state and magnonic state by changing the cavity–magnon coupling strength. With the numerical simulation, we quantitatively show that the photonic, magnonic and magnon-to-photon state transfers can be achieved with high fidelity in the cavity–magnon system. Spectacularly, three different types of quantum state transfer schemes can be even transformed into each other in a controllable fashion. The Su–Schrieffer–Heeger model based on the cavity–magnon system provides us a tunable platform to engineer the transport of photon and magnon, which may have potential applications in topological quantum processing.

Keywords: topological state transfer, cavity–magnon system, high fidelity

PACS: 03.65.Vf, 03.67.–a, 05.60.Gg **DOI:** 10.1088/1674-1056/acc3f6

1. Introduction

Quantum state transfer (QST) is of major interest in physics with potential applications in quantum information processing.[1–26] Several schemes have been proposed to discuss QST theoretically and experimentally, such as cavity electromechanical systems,[20–22] spin chains,[5,6,17,23,24] quantum dots,[25,26] and trapped ions systems.[2] Among these studies, it can be found that the major requirement of QST protocols is robust. To this regard, the topological QST has attracted much attention because the topology can provide invariance against sizable imperfections in quantum information processing.[27–36] The Su–Schrieffer–Heeger (SSH) model is a promising platform to analyze the topological QST due to its structural simplicity and abundant physical insight.[37–40] Concretely, the robust QST assisted by Landau–Zener tunneling has been reported.[41] In addition, Dlaska *et al.*[42] have displayed the robust QST via topologically protected edge pumping in a two-dimensional topological spin system. Subsequently, in superconducting qubit chain[43] and superconducting flux qubit chain,[44] robust QSTs via topological edge states have been realized. Especially, Qi *et al.*[45] studied the one-dimensional modulated SSH chain composed of small optomechanical lattice to implement photonic and phononic topological state transfer.

On the other hand, cavity optomagnonic systems have been extensively investigated recently, which provide a new platform for studying quantum effect.[46–56] Magnon, the collective spin excitation for ferromagnetic material, can realize the strong (even ultrastrong) couplings with cavity photons.[46,51] Further, the yttrium iron garnet (YIG) sphere is often used as the ferromagnetic material for the experiment, and this has been characterized by high collective spin excitation density and low dissipation.[57,58] In addition, the strong coupling between cavity photons and magnons has been observed at low, room and high temperatures experimentally.[59,60] Moreover, compared to cavity-optomechanical systems, the cavity optomagnonic system possesses a long coherence time and intrinsically good tunability.[46] Based on the merits of the cavity optomagnonic system, it is also expected to implement the potential application in quantum information networks,[55] quantum sensing,[61,62] and magnon dark modes in magnon-gradient memories.[63]

In this study, in terms of these excellent properties of cavity–magnon systems, a new protocol for implementing high-fidelity QST is proposed. By putting YIG spheres into the cavity, a one-dimensional cavity–magnon system is constructed. We analytically find that the system is equivalent to the generalized SSH model. Then, through adiabatical ramping of the cavity–magnon couplings, we find that the topological edge state can be obtained and used as topologically protected quantum channels to realize the photonic, magnonic and magnon-to-photon state transfers. Our results numerically demonstrate that the process of QST is accomplished with high fidelity via the gap state because of the topological protection. More spectacularly, we unveil that different

†Corresponding author. E-mail: tanlei@lzu.edu.cn

© 2023 Chinese Physical Society and IOP Publishing Ltd

kinds of transition channels can be switched to each other. Our results provide a scheme for implementing the QST in a cavity–magnon system, which will offer potential applications for quantum information processing.

The paper is organized as follows. In Section 2 we present the theoretical model of the cavity–magnon system, which can be mapped into a tight-binding SSH model. Section 3 is devoted to researching the photonic state transfer in the cavity–magnon system. In Section 4 we explore the magnonic state transfer and magnon-to-photon state transfer. Finally, the conclusions are presented in Section 5.

2. The cavity–magnon system

We consider a one-dimensional cavity–magnon system composed of $N+1$ cavity modes[64–66] and N YIG spheres (red spheres), as depicted in Fig. 1.

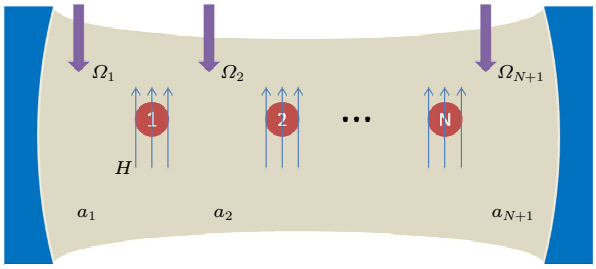


Fig. 1. The diagrammatic sketch of a one-dimension cavity–magnon system consisting of $N+1$ cavity modes and N YIG spheres. Here $a_1, a_2, \ldots, a_{N+1}$ represent cavity modes which are pumped by the laser fields shown with purple arrows. YIG spheres (red spheres) are placed at the cavity and in a uniform bias magnetic field H.

Each cavity field is driven by a laser field with strength Ω_n $(n = 1, 2, \ldots, N+1)$. Specifically, the system reads

$$\begin{aligned} H_1 = &\sum_{n=1}^{N+1} (\omega_{a,n} a_n^\dagger a_n + \Omega_n a_n^\dagger e^{-i\omega_d t} + \Omega_n^* a_n e^{i\Omega_d t}) \\ &+ \sum_{n=1}^{N} \Omega_{m,n} m_n^\dagger m_n + \sum_{n=1}^{N} [g_n (a_n^\dagger + a_n)(m_n + m_n^\dagger) \\ &+ g_n' (a_{n+1}^\dagger + a_{n+1})(m_n + m_n^\dagger) + J(a_{n+1}^\dagger a_n + a_n^\dagger a_{n+1})], \end{aligned} \tag{1}$$

where $a_n^\dagger$ (a_n) and $m_n^\dagger$ (m_n) are the photonic and magnonic creation (annihilation) operators. The first term is the free energy of the cavity fields with frequencies $\Omega_{a,n}$ and driving laser with frequency Ω_d. The second term is the free energy of the magnons with frequencies $\Omega_{m,n}$. The last term represents the coupling between the adjacent cavity modes and the magnons through magnetic dipole coupling the cavity modes, in which the coupling strengths are g_n, g_n' and J, respectively. Then, by using a rotating transformation with the external driving frequency Ω_d and utilizing the rotation-wave approximation,[67] the total Hamiltonian H_1 becomes

$$\begin{aligned} H_2 = &\sum_{n=1}^{N+1} (\Delta_{a,n} a_n^\dagger a_n + \Omega_n a_n^\dagger + \Omega_n^* a_n) + \sum_{n=1}^{N} \Delta_{m,n} m_n^\dagger m_n \\ &+ \sum_{n=1}^{N} [g_n (a_n^\dagger m_n + a_n m_n^\dagger) + g_n' (a_{n+1}^\dagger m_n + a_{n+1} m_n^\dagger) \\ &+ J(a_{n+1}^\dagger a_n + a_n^\dagger a_{n+1})], \end{aligned} \tag{2}$$

where $\Delta_{a,n} = \Omega_{a,n} - \Omega_d$ $(\Delta_{m,n} = \Omega_{m,n} - \Omega_d)$ is the detuning between the cavity mode (magnon modes) and the external lasers. Subsequently, we utilize the standard linearization process, i.e., the operators a_n and m_n are replaced by $a_n = \langle a_n \rangle + \delta a_n = \alpha_n + \delta a_n$ and $m_n = \langle m_n \rangle + \delta m_n = \beta_n + \delta m_n$, respectively.[45,68] Through taking out "δ" for all fluctuation operators δa_n and δm_n, the Hamiltonian is given by

$$\begin{aligned} H_3 = &\sum_{n=1}^{N+1} \Delta_{a,n} a_n^\dagger a_n + \sum_{n=1}^{N} \Delta_{m,n} m_n^\dagger m_n \\ &+ \sum_{n=1}^{N} g_n [(a_n^\dagger m_n + a_n m_n^\dagger) + g_n' (a_{n+1}^\dagger m_n + a_{n+1} m_n^\dagger) \\ &+ J(a_{n+1}^\dagger a_n + a_n^\dagger a_{n+1})]. \end{aligned} \tag{3}$$

We further implement another rotating transformation with respect to $\Delta_{a,n} a_n^\dagger a_n$ and $\Delta_{m,n} m_n^\dagger m_n$, i.e.,

$$U = \exp\left[-i\left(\sum_{n=1}^{N+1} \Delta_{a,n} a_n^\dagger a_n + \sum_{n=1}^{N} \Delta_{m,n} m_n^\dagger m_n\right)\right]. \tag{4}$$

Then, the Hamiltonian becomes

$$\begin{aligned} H_4 = &\sum_{n=1}^{N} [g_n (a_n^\dagger m_n e^{i(\Delta_{a,n} - \Delta_{m,n})t} + a_n m_n^\dagger e^{-i(\Delta_{a,n} - \Delta_{m,n})t}) \\ &+ g_n' (a_{n+1}^\dagger m_n e^{i(\Delta_{a,n} - \Delta_{m,n})t} + a_{n+1} m_n^\dagger e^{-i(\Delta_{a,n} - \Delta_{m,n})t}) \\ &+ J(a_{n+1}^\dagger a_n + a_n^\dagger a_{n+1})]. \end{aligned} \tag{5}$$

When the parameters satisfy $\Delta_{a,n} = \Delta_{m,n}$, the Hamiltonian ultimately becomes

$$\begin{aligned} H_5 = &\sum_{n=1}^{N} [g_n (a_n^\dagger m_n + a_n m_n^\dagger) + g_n' (a_{n+1}^\dagger m_n + a_{n+1} m_n^\dagger) \\ &+ J(a_{n+1}^\dagger a_n + a_n^\dagger a_{n+1})]. \end{aligned} \tag{6}$$

Remarkably, if $J = 0$, the Hamiltonian H_5 only possesses the interactions between the adjacent cavity mode and the magnonic mode. It means that the one-dimensional cavity–magnon system can be transformed into a generalized SSH model physically. Next, in the numerical calculation, we use parameters from the recent experimental and theoretical studies on a hybrid system.[69,70] These values are $\Omega_{a,n}/2\pi =$ 10 GHz, $\Omega_{m,n}/2\pi = 10$ GHz and $\Omega_d/2\pi = 10$ GHz.

3. Photonic state transfer in the cavity–magnon system

We first consider the standard SSH model, i.e., $J = 0$. Hamiltonian (6) becomes

$$H_6 = \sum_{n=1}^{N} [g_n (a_n^\dagger m_n + a_n m_n^\dagger) + g_n' (a_{n+1}^\dagger m_n + a_{n+1} m_n^\dagger)]. \tag{7}$$

Here, we have taken $g_n = g$ and $g'_n = g'$, and used $g = g_0(1-\cos\theta)$ and $g' = g'_0(1+\cos\theta)$, in which θ is the modulated parameter in the range of $\theta \in [0, 2\pi]$. The edge states are exponentially localized at the boundaries. Specifically, in a single excitation subspace, the wave function has the form $|\Psi\rangle(\theta) = \sum_n \lambda^n(\alpha a_n^\dagger + \beta m_n^\dagger)|G\rangle$,[43] in which $|G\rangle = |0\rangle_{a_1} \otimes |0\rangle_{m_1} \cdots \otimes |0\rangle_{a_{N+1}} = |0,0,0,\ldots,0\rangle$ and λ denotes the localization indexes. Then, the eigenvalue equation can be acquired as follows:

$$g\lambda^n \beta a_n^\dagger|G\rangle + g'\lambda^{n+1}\alpha m_n^\dagger|G\rangle + g\lambda^n \alpha m_n^\dagger|G\rangle + g'\lambda^{n-1}\beta a_n^\dagger|G\rangle = E\lambda^n(\alpha a_n^\dagger + \beta m_n^\dagger). \tag{8}$$

Therefore, the zero-energy edge state wavefunction can be derived as

$$|\Psi\rangle = \sum_n \left(-\frac{g}{g'}\right)^n a_n^\dagger|G\rangle. \tag{9}$$

Equation (9) analytically demonstrates that the edge state occupies near the left boundary when $\theta \in (0, \frac{\pi}{2})$ and $\theta \in (\frac{3\pi}{2}, 2\pi)$, while $\theta \in (\frac{\pi}{2}, \frac{3\pi}{2})$, it is localized near the right boundary. Note that both the left and right sites belong to the cavity fields, which means that the photon is transferred. To further visualize the above analytical expression, we plot the distribution of the zero-energy mode, as shown in Fig. 2(b). One can find that the distribution of the zero-energy mode is well consistent with the analytical calculation. Concretely, the cavity–magnon coupling strength becomes $g = 0$ ($g' = 0$) when $\theta = 0$ ($\theta = \pi$), which induces that the leftmost (rightmost) cavity mode is decoupled from the rest of the cavity–magnon system. Therefore, the edge states become $|\psi_0\rangle = |1\rangle_{a_1} \otimes |0\rangle_{m_1} \cdots \otimes |0\rangle_{a_{N+1}} = |1,0,0,\ldots,0\rangle$ and $|\psi_\pi\rangle = |0\rangle_{a_1} \otimes |0\rangle_{m_1} \cdots \otimes |1\rangle_{a_{N+1}} = |0,0,0,\ldots,1\rangle$. Then, the above result provides some important information that we can achieve a photonic topological state transfer between the first and the last cavity fields assisted by the zero-energy mode via varying the periodic parameter θ from 0 to π.

Here, let us assume that the periodic parameter θ is varied in time, namely, $\theta(t) = \Omega t$, with Ω being the varying rate.[43] If the initial state is prepared in the photonic left edge state $|\psi_0\rangle = |1,0,0,\ldots,0\rangle$, the photonic right edge state can be obtained through the evolution of the time-dependent Hamiltonian $\mathrm{i}\frac{\partial}{\partial t}|\Psi_t\rangle = H(\theta_t)|\Psi_t\rangle$. Further, the fidelity of this evolution process $F = |\langle\psi_\pi|\Psi_f\rangle|$ can be numerically calculated as shown in Fig. 2(c). Affirmatively, the fidelity is maintained as the value of unity over a large range. For example, we can choose $\Omega = 0.03$ to ensure the photonic state transfer from $|\psi_0\rangle$ to $|\psi_\pi\rangle$ with high fidelity. The coupling strength of cavity–magnon can reach $g/2\pi = g'/\pi = 2$ GHz.[54] This strong coupling strength corresponds to the time of QST being $t = \pi/\Omega = 8.3$ ns, which means that the time is particularly short compared with the decay time of the magnon.[46]

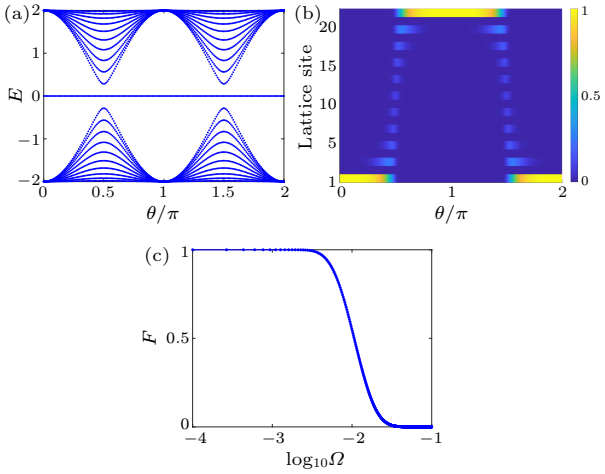


Fig. 2. (a) Energy spectra of the cavity–magnon system with $g_0/2\pi = g'_0/2\pi = 1$ MHz and $J = 0$. A zero-energy state always exists. (b) The corresponding state distribution of the zero-energy state. (c) The fidelity of the state transfer between $|\psi_0\rangle$ to $|\psi_\pi\rangle$ versus the varying rate of Ω.

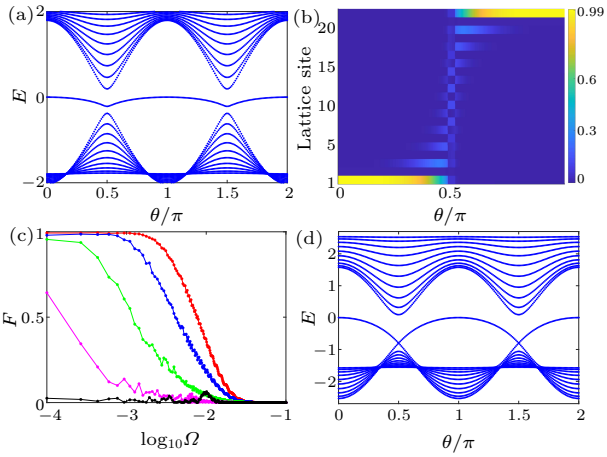


Fig. 3. (a) The energy spectra of the cavity–magnon system with $g_0/2\pi = g'_0/2\pi = 1$ MHz and $J/2\pi = 0.125$ MHz. A gap state always exists. (b) The corresponding state distribution. (c) The fidelity with $J/2\pi = 0.125$ MHz (red line), 0.2 MHz (blue line), 0.3 MHz (green line), 0.4 MHz (pink line) and 0.5 MHz (black line). (d) The energy spectrum with $J/2\pi = 0.5$ MHz. Here, the lattice size is $L = 21$.

Further, we consider the case of $J \neq 0$. In Figs. 3(a) and 3(b), the energy spectrum and the corresponding gap state distribution can be displayed with $J/2\pi = 0.125$ MHz. Clearly, this gap state is not the zero mode, and the energy gap is still nonzero. In other words, this state can also be viewed as a channel to realize QST. Correspondingly, as shown in Fig. 3(b), the photon prepared initially in the first cavity mode can be transferred into the last cavity mode finally. In Fig. 3(c), we exhibit the fidelity of this evolution process once again, in which the red line stands for $J/2\pi = 0.125$ MHz. Obviously, the fidelity $F > 99\%$ when $-4 < \log_{10}\Omega < -2.5$, i.e., the photon state can be transferred almost perfectly. In addition, we also calculate the fidelity for some values of J. It can be shown that the situation becomes different when J continues to increase but less than g. Concretely, with $J/2\pi = 0.5$ MHz (the black line), the fidelity is close to zero. Physically, it can be explained that the large J completely destroys the original state

transfer channel, as shown in Fig. 3(d), with the gap states coming into the bulk.

So far, we have found that the photonic state can be transferred across the chain with high fidelity. Next, we explore what new QST scheme will occur in our cavity–magnon system.

4. Magnonic state transfer and magnon-to-photon state transfer

In this section, we discuss other state transfer protocols in the cavity–magnon system by changing the coupling strength between adjacent cavity modes J and the intracell hopping strength g_0.

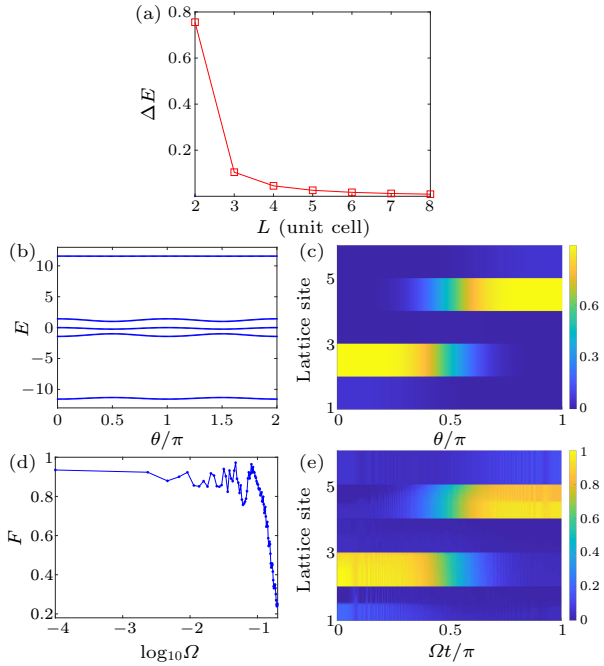


Fig. 4. (a) Energy gap (the gap state and the low band) ΔE versus the length of the chain. (b) The energy spectra of the cavity–magnon system. A gap state always exists. (c) The corresponding state distribution of the gap state. (d) The fidelity between $|\psi_0\rangle = |0,1,0,0,0\rangle$ and $|\psi_\pi\rangle = |0,0,0,1,0\rangle$. (e) The state transfer process corresponding to $\Omega = 3\times10^{-4}$. Other parameters are $g_0/2\pi = g_0'/2\pi = 1$ MHz and $J/2\pi = 8$ MHz.

Magnonic state transfer As we all know, the closure of the energy gap marks that the gap state does not exist. In Fig. 4(a), we plot the energy gap ΔE versus the length of the chain with $g_0/2\pi = g_0'/2\pi = 1$ MHz and $J/2\pi = 8$ MHz. One can find that the energy gap tends to be narrow with the increasing number of unit cells. Therefore, in order to better elucidate the state transition process, the length of the following cavity–magnon system can be taken as $L = 5$.

To explore the QST, as shown in Fig. 4(b), the energy spectrum is obtained. It can be shown that the shape of the gap state is wavy-like, which implies that a new channel realizing another type of state transfer may be apparent. In order to demonstrate this assertion, we plot the state distribution in Fig. 4(c). Obviously, corresponding to $\theta = 0$, the gap state is localized near the first YIG sphere, while it is located near the second YIG sphere when $\theta = \pi$. These results show that the gap state becomes a new state transfer channel between the magnonic states of $|\psi_0\rangle = |0,1,0,0,0\rangle$ and $|\psi_\pi\rangle = |0,0,0,1,0\rangle$. The numerical results mentioned above can be understood physically as follows. The larger adjacent cavity coupling strength J makes the original three cavity modes regarded as a cavity field.[45] Therefore, this system can realize state transfer between magnons. To further confirm this behavior, we numerically simulate the fidelity of the magnonic state transfer in Fig. 4(d). We find that, when the ramping speed $\log_{10}\Omega < -2.3$, the state transfer between $|\psi_0\rangle = |0,1,0,0,0\rangle$ and $|\psi_\pi\rangle = |0,0,0,1,0\rangle$ can be realized with high fidelity. We also depict the state transfer process through the evolution of the time-dependent Schrödinger equation when $\Omega = 3\times10^{-4}$ in Fig. 4(e). Obviously, the state transfer between $|\psi_0\rangle = |0,1,0,0,0\rangle$ and $|\psi_\pi\rangle = |0,0,0,1,0\rangle$ can indeed be implemented.

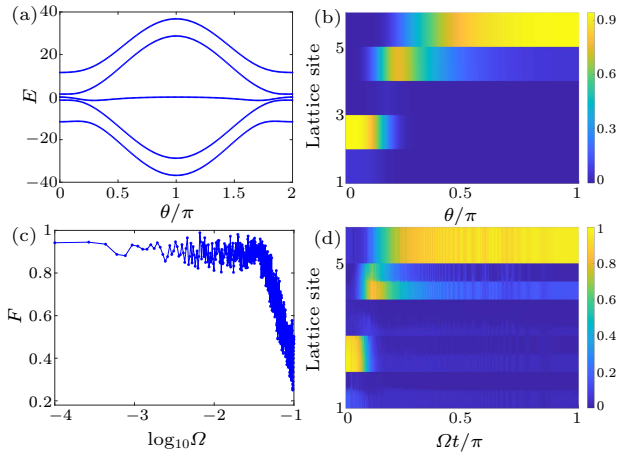


Fig. 5. (a) Energy spectra of the cavity–magnon system with $g_0/2\pi = 16$ MHz, $g_0'/2\pi = 1$ MHz and $J/2\pi = 8$ MHz. (b) The corresponding state distribution of the gap state. (c) The fidelity between $|\psi_0\rangle = |0,1,0,0,0\rangle$ and $|\psi_\pi\rangle = |0,0,0,0,1\rangle$. (d) The state transfer process corresponding to $\Omega = 0.001$.

Magnon-to-photon state transfer We have demonstrated that the magnonic state transfer is applicable when $g_0/2\pi = g_0'/2\pi = 1$ MHz and $J/2\pi = 8$ MHz. Then, what will happen if we change the value of g_0? We can now take $g_0/2\pi = 16$ MHz. The energy spectrum and the corresponding gap state distribution are plotted in Figs. 5(a) and 5(b). One can find that the gap state is occupied near the second site when $\theta = 0$, whereas it is localized near the last site when $\theta = \pi$. In other words, it can realize the transfer from a magnonic state $|\psi_0\rangle = |0,1,0,0,0\rangle$ to a photon state $|\psi_\pi\rangle = |0,0,0,0,1\rangle$ by dint of this channel. Similarly, the fidelity of the state transfer versus the ramping speed Ω can be shown in Fig. 5(c). It can be found that when $-4 < \log_{10}\Omega < -3$, the fidelity $F > 90\%$. A small Ω is required to meet the adiabatic evolution condition since the energy gap is narrow at this point. Moreover, to make the results more intuitive, in Fig. 5(d), the numerical result reveals exactly that the state transfer between

the magnonic state $|\psi_0\rangle = |0,1,0,0,0\rangle$ and the photon state $|\psi_\pi\rangle = |0,0,0,0,1\rangle$ with $\Omega = 0.001$.

From Sections 3 and 4, we can realize that the photonic, magnonic and magnon-to-photon state transfers can be fulfilled by the gap state. In detail, the photonic state and magnonic state transfer processes can only be adjusted by the coupling strength between adjacent cavity modes J appropriately. Analogously, the magnonic and magnon-to-photon state transfer processes can be regulated by the intracell hopping g_0. Therefore, the three different types of quantum state transfer schemes can be switched to each other by designing parameters suitably for the considered cavity–magnon system.

5. Conclusions

In summary, we have proposed an innovative scheme to realize high-fidelity quantum state transfer based on the topologically protected edge state in a cavity–magnon system. We analytically find that the cavity–magnon system can be transformed into the generalized SSH model. It can be found that the edge state can be employed as a quantum channel to realize the photonic, magnonic and magnon-to-photon state transfer with high fidelity. In addition, one can find that the photonic, magnonic and magnon-to-photon state transfer can be controlled by changing the value of the parameter appropriately. The results obtained here provide a scheme for realizing the QST in a cavity magnonic system, which will provide valuable insight into topological quantum information processing.

Experimentally, it is a mature technology that a coupling magnon-photon system can be engineered.[56,71–73] Moreover, the multimode coupling in cavity quantum electrodynamics has also been realized.[65,74] In addition, based on Ref. [75], the behavior of a large number of YIG spheres coupled to cavity mode is tested. Specifically, this setup, consisting of ten 2.1-mm-diameter YIG spheres coupled to a copper microwave cavity, is used for studying the behavior of the hybrid system at temperatures of mK. Therefore, the theoretical model we proposed here may be experimentally realized with the development of experimental technology.

Acknowledgments

This work was supported by the National Natural Science Foundation of China (Grant Nos. 11874190, 61835013, and 12047501) and the Supercomputing Center of Lanzhou University.

References

[1] Saffman M, Walker T G and Mølmer K 2010 *Rev. Mod. Phys.* **82** 2313
[2] Duan L M and Monroe C 2010 *Rev. Mod. Phys.* **82** 1209
[3] Suter D and Álvarez G A 2016 *Rev. Mod. Phys.* **88** 041001
[4] Kay A 2009 *Phys. Rev. A* **79** 042330
[5] Paganelli S, Lorenzo S, Apollaro T J G, Plastina F and Giorgi G L 2013 *Phys. Rev. A* **87** 062309
[6] Lorenzo S, Apollaro T J G, Paganelli S, Palma G M and Plastina F 2015 *Phys. Rev. A* **91** 042321
[7] Plenio M B, Hartley J and Eisert J 2004 *New J. Phys.* **6** 36
[8] Vijay S and Fu L 2016 *Phys. Rev. B* **94** 235446
[9] Stannigel K, Rabl P, Sørensen A S, Lukin M D and Zoller P 2011 *Phys. Rev. A* **84** 042341
[10] Chen Q and Feng M 2010 *Phys. Rev. A* **82** 052329
[11] Zhang Z T and Yu Y 2013 *Phys. Rev. A* **87** 032327
[12] Li D X and Shao X Q 2018 *Phys. Rev. A* **98** 062338
[13] Stannigel K, Komar P, Habraken S J M, Bennett S D, Lukin M D, Zoller P and Rabl P 2012 *Phys. Rev. Lett.* **109** 013603
[14] Rips S and Hartmann M J 2013 *Phys. Rev. Lett.* **110** 120503
[15] Chen J, Nurdin H I and Yamamoto N 2020 *Phys. Rev. Appl.* **14** 024065
[16] Cirac J I, Zoller P, Kimble H J and Mabuchi H 1997 *Phys. Rev. Lett.* **78** 3221
[17] Christandl M, Datta N, Ekert A and Landahl A J 2004 *Phys. Rev. Lett.* **92** 187902
[18] Wang Y D and Clerk A A 2012 *Phys. Rev. Lett.* **108** 153603
[19] Zhang J, Peng K and Braunstein S L 2003 *Phys. Rev. A* **68** 013808
[20] Zheng S B and Guo G C 2000 *Phys. Rev. Lett.* **85** 2392
[21] Yang C P, Chu S I and Han S 2003 *Phys. Rev. A* **67** 042311
[22] Yang C P, Chu S I and Han S 2004 *Phys. Rev. Lett.* **92** 117902
[23] Bose S 2003 *Phys. Rev. Lett.* **91** 207901
[24] Yao N Y, Jiang L, Gorshkov A V, Gong Z X, Zhai A, Duan L M and Lukin M D 2011 *Phys. Rev. Lett.* **106** 040505
[25] Brandes T and Vorrath T 2002 *Phys. Rev. B* **66** 075341
[26] He Y, He Y M, Wei Y J, Jiang X, Chen K, Lu C Y, Pan J W, Schneider C, Kamp M and Höfling S 2017 *Phys. Rev. Lett.* **119** 060501
[27] Hasan M Z and Kane C L 2010 *Rev. Mod. Phys.* **82** 3045
[28] Qi X L and Zhang S C 2011 *Rev. Mod. Phys.* **83** 1057
[29] Chiu C K, Teo J C Y, Schnyder A P and Ryu S 2016 *Rev. Mod. Phys.* **88** 035005
[30] Bansil A, Lin H and Das T 2016 *Rev. Mod. Phys.* **88** 021004
[31] Shen S Q 2012 *Topological Insulators: Dirac Equation in Condensed Matters*. In: *Springer Series in Solid-State Sciences* vol 174
[32] Wu Q, Du L and Sacksteder V E 2013 *Phys. Rev. B* **88** 045429
[33] Chen L, Wang Z F and Liu F 2013 *Phys. Rev. B* **87** 235420
[34] Paananen T and Dahm T 2013 *Phys. Rev. B* **87** 195447
[35] Malki M and Uhrig G S 2017 *Phys. Rev. B* **95** 235118
[36] Brouwer P W, Duckheim M, Romito A and von Oppen F 2011 *Phys. Rev. B* **84** 144526
[37] Li L, Xu Z and Chen S 2014 *Phys. Rev. B* **89** 085111
[38] Di Liberto M, Recati A, Carusotto I and Menotti C 2016 *Phys. Rev. A* **94** 062704
[39] Bao X X, Guo G F, Du X P, Gu H Q and Tan L 2021 *J. Phys.: Condens. Matter* **33** 185401
[40] Guo G F, Bao X X and Tan L 2021 *New J. Phys.* **23** 123007
[41] Longhi S, Giorgi G L and Zambrini R 2019 *Adv. Quantum Technol.* **2** 1800090
[42] Dlaska C, Vermersch B and Zoller P 2017 *Quantum Sci. Technol.* **2** 015001
[43] Mei F, Chen G, Tian L, Zhu S L and Jia S 2018 *Phys. Rev. A* **98** 012331
[44] Zheng L N, Qi L, Cheng L Y, Wang H F and Zhang S 2020 *Phys. Rev. A* **102** 012606
[45] Qi L, Wang G L, Liu S, Zhang S and Wang H F 2020 *Opt. Lett.* **45** 2018
[46] Lachance-Quirion D, Tabuchi Y, Gloppe A, Usami K and Nakamura Y 2019 *Appl. Phys. Express* **12** 070101
[47] Zhao C, Li X, Chao S, Peng R, Li C and Zhou L 2020 *Phys. Rev. A* **101** 063838
[48] Osada A, Hisatomi R, Noguchi A, Tabuchi Y, Yamazaki R, Usami K, Sadgrove M, Yalla R, Nomura M and Nakamura Y 2016 *Phys. Rev. Lett.* **116** 223601
[49] Gao Y P, Liu X F, Wang T J, Cao C and Wang C 2019 *Phys. Rev. A* **100** 043831
[50] Haigh J A, Nunnenkamp A, Ramsay A J and Ferguson A J 2016 *Phys. Rev. Lett.* **117** 133602
[51] Zhang X, Zou C L, Jiang L and Tang H X 2014 *Phys. Rev. Lett.* **113** 156401
[52] Zhang X, Zhu N, Zou C L and Tang H X 2016 *Phys. Rev. Lett.* **117** 123605
[53] Tabuchi Y, Ishino S, Ishikawa T, Yamazaki R, Usami K and Nakamura Y 2014 *Phys. Rev. Lett.* **113** 083603
[54] Goryachev M, Farr W G, Creedon D L, Fan Y, Kostylev M and Tobar M E 2014 *Phys. Rev. Appl.* **2** 054002
[55] Li J, Wang Y P, Wu W J, Zhu S Y and You J Q 2021 arXiv:2108.11156 [quant-ph]

[56] Wang Y P, Zhang G Q, Zhang D, Li T F, Hu C M and You J Q 2018 *Phys. Rev. Lett.* **120** 057202
[57] Chumak A V, Vasyuchka V I, Serga A A and Hillebrands B 2015 *Nat. Phys.* **11** 3347
[58] Tan H and Li J 2021 *Phys. Rev. Res.* **3** 013192
[59] Xiao Y, Yan X H, Zhang Y, Grigoryan V L, Hu C M, Guo H and Xia K 2019 *Phys. Rev. B* **99** 094407
[60] Liu Z X, Xiong H and Wu Y 2019 *IEEE Acc.* **7** 57047
[61] Cao Y and Yan P 2019 *Phys. Rev. B* **99** 214415
[62] Ebrahimi M S, Motazedifard A and Harouni M B 2021 *Phys. Rev. A* **103** 062605
[63] Zhang X F, Zou C L, Zhu N, Marquardt F, Jiang L and Tang H X 2015 *Nat. Commun.* **6** 9914
[64] Strack P and Sachdev S 2011 *Phys. Rev. Lett.* **107** 277202
[65] Sundaresan N M, Liu Y, Sadri D, Szöcs L J, Underwood D L, Malekakhlagh M, Türeci H E and Houck A A 2015 *Phys. Rev. X* **5** 021035
[66] Torggler V, Krämer S and Ritsch H 2017 *Phys. Rev. A* **95** 032310
[67] Xu Y J, Wang S S, Chen M R and Liao Q H 2019 *Laser Phys.* **29** 065202
[68] Xu X W, Zhao Y J, Wang H, Chen A X and Liu Y X 2022 *Front. Phys.* **9** 813801
[69] Zhang X, Zou C L, Jiang L and Tang H X 2016 *Sci. Adv.* **2** e1501286
[70] Ullah K, Naseem M T and Müstecaplioğlu O E 2020 *Phys. Rev. A* **102** 033721
[71] van Oosten D, van der Straten P and Stoof H T C 2001 *Phys. Rev. A* **63** 053601
[72] Wang Y P, Zhang G Q, Zhang D, Luo X Q, Xiong W, Wang S P, Li T F, Hu C M and You J Q 2016 *Phys. Rev. B* **94** 224410
[73] Buks E, Brookes P, Ginossar E, Deng C, Orgiazzi J L F X, Otto M and Lupascu A 2020 *Phys. Rev. A* **102** 043716
[74] Kelly S P, Rey A M and Marino J 2021 *Phys. Rev. Lett.* **126** 133603
[75] Crescini N, Braggio C, Carugno G, Ortolan A and Ruoso G 2021 *Phys. Rev. B* **104** 064426